HEFAT2014
10th International Conference on Heat Transfer, Fluid Mechanics and Thermodynamics
14 – 16 July 2014
Orlando, Florida

LATTICE BOLTZMANN SIMULATION OF A STORAGE TANK WITH AN IMMERSED TUBE BUNDLE HEAT EXCHANGER

Yan Su
Department of Electromechanical Engineering,
Faculty of Science and Technology,
University of Macau, Taipa, Macau
E-mail: yansu@umac.mo

ABSTRACT

A rectangular storage tank with an immersed cylindrical tube bundle heat exchanger has been simulated by Lattice Boltzmann Method (LBM). The details of transient temperature distributions and flow streamlines in the nearby field of each tube are clearly demonstrated as well as the complexity of the overall flow field and the extent of the mixing during discharge. The LBM makes the directly simulation possible and the computational speed is increased comparing to a conventional porous medium model simulation. The transient averaged Nusselt numbers of the tube bundle have been obtained, which can also be applied in other applications such as numerical simulations of porous medium models.

NOMENCLATURE

c_p	[J/kg-K]	Thermal capacity of water
$\boldsymbol{c}$	[m/s]	Lattice velocity vector
f	[kg/m^3]	Density distribution function
g	[K/m^3]	Temperature distribution function
$\mathbf{g}$	[m/s^2]	Gravity acceleration
L_x	[m]	Width of the storage tank
L_y	[m]	Height of the storage tank
t	[s]	Time
U	[m/s]	Velocity scale
x	[m]	Cartesian axis direction
y	[m]	Cartesian axis direction

Special characters

ν	[m/s^2]	Kinematic viscocity
α	[m]	Thermal dispersivity
ρ	[kg/m^3]	Density
ℓ	[m]	Lattice length scale
Δx	[m]	Mesh size in x direction
Δy	[m]	Mesh size in y direction

Subscripts

d	Microscopic length scale
L	Macroscopic length scale

INTRODUCTION

Fluid flow and heat transfer of tube bundles immersed in solar storage tank have been studied widely for their importance on the Engineering applications [1]. In early time, either experimental study or numerical study using a small unit to present the whole tube bundle has been investigated. It would be time and space consuming to employ the conventional methods such as finite difference, finite element, and control volume methods to simulate the transient flow and heat transfer of the tube bundle heat exchanger. This is because the computation speed and accuracy of these methods are highly dependent on convergence speed and accuracy of the Poisson solver [2]. Then, porous medium models are applied to study the overall effects based on a representative element volume (REV) [1, 3].

Recently, one of the state-of-the-art methods, Lattice Boltzmann Method (LBM), has been proposed to increase the simulation speed and also to adapt to complex geometry domains. A lot of study of LBM for natural and mixed convection inside a closed enclosure driven by top lid and buoyancy force have been carried out by introducing a body force term into the momentum equation for macroscopic Reynolds number up to and the macroscopic Rayleigh number up to [4]-[7]. Also conjugate heat transfer can be solved easily with LBM method by modification of the relaxation time in the energy equation [8].

However, for the present study our Rayleigh numbers would be substantially larger than those in the above literature. Moreover, the conventional LBM method with parameters based on real units cannot explicitly show the effects of the dimensionless parameters and mesh size on computational accuracy. In order to overcome the above limitations of the conventional LBM with units, this paper develops a numerical model based on LBM for the solar storage tank with a immersed tube bundle heat exchanger. Compared to the conventional LBM, the proposed method can clearly reveal the relations of the macroscopic, microscopic, and mesoscopic length scales.

NUMERICAL MODEL

As shown in Fig. 1, the tilted heat storage tank can be modeled as a fluid enclosure with a randomly distributed 240 tube bundle heat exchanger near the top. Two kinds of distribution based on loosely distributed tubes and compacted tubes will be investigated in the present study. Figure 1(a) shows a loosely distributed tube bundle, while Fig. (b) shows a compacted tube bundle with the same number of tubes. During the discharge procedure, the initial temperature of the tank is at a uniform high value T_0. The heat will be taken away by the immersed small tubes with time going on. The gravity force is in the -30^o direction start from the x axis.

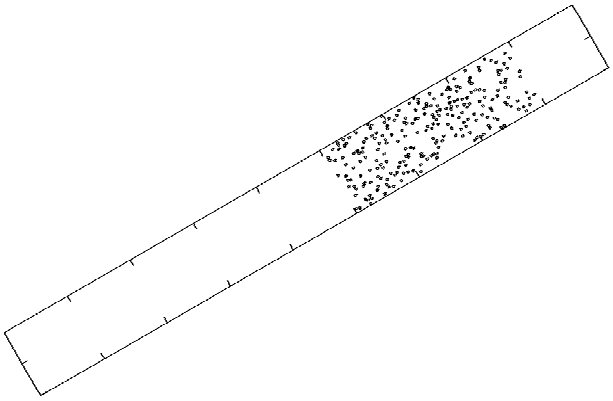

(a)

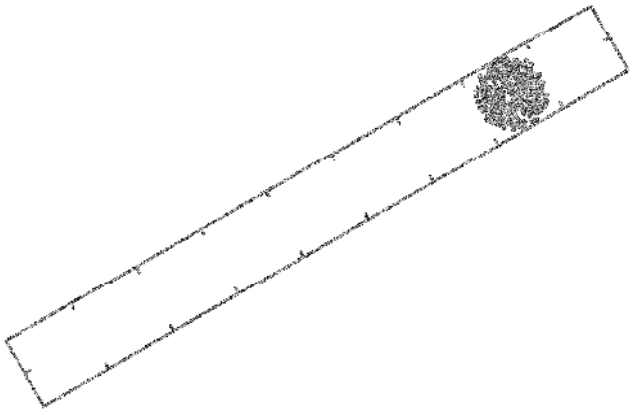

(b)

Figure 1 Sketch of the randomly distributed tubes in mid of the storage tank: (a) loosely distributed 240 tubes (b) compacted 240tubes

The LBM is applied to simulate the transient natural convection inside the solar storage tank with the 240 tube-bundle heat exchanger. D2Q9 scheme is chosen in the present study because previous studies show that two dimensional simulations can capture the heat transfer coefficient as well as the three dimensional study [3]. For the present problem, the macroscopic length scale is the gap height of the channel, H. The fluid domain is meshed in size of $n \times m$, then the mesh size for both the solid and fluid part is $n \times m$. The mesoscopic length scale, i.e. the lattice mesh size and the length scale for the present numerical study, $\ell = \Delta x = \Delta y = L_y/m = L_x/n$. The temperature scale is the initial temperature difference between the storage fluid and the tube wall ΔT, and the reference temperature is the fluid temperature in the mid of the storage tank T_{ref}. The velocity scale for the natural convection is $U = \sqrt{g\beta\Delta TL}$.

The corresponding macroscopic Rayleigh number is based on the macroscopic length scale, i.e. width of the tank L,

$$Ra_L = \frac{g\beta\Delta TL^3}{\nu_f \alpha_f} \tag{1}$$

The microscopic Rayleigh number is based on the microscopic length scale, i.e. the tube diameter d,

$$Ra_d = \frac{g\beta\Delta Td^3}{\nu_f \alpha_f} \tag{2}$$

Denote f as dimensionless density distribution function and g as the dimensionless temperature distribution function, we can obtain the following Lattice Boltzmann Equations (LBE) for the momentum equation and heat transfer equation respectively:

$$f_k(\mathbf{x}+\mathbf{c}_k\Delta t, t+\Delta t) = f_k(\mathbf{x},t) - \frac{\Delta t}{\tau_f}\left(f_k(\mathbf{x},t) - f_k^{eq}(\mathbf{x},t)\right) + F_k \tag{3}$$

$$g_k(\mathbf{x}+\mathbf{c}_k, t+1) = g_k(\mathbf{x},t) - \frac{\Delta t}{\tau_g}\left(g_k(\mathbf{x},t) - g_k^{eq}(\mathbf{x},t)\right) + Q_k \tag{4}$$

Then, the respective dimensionless density, velocity, and temperature can be obtained as follows:

$$\rho = \sum_k f_k, \tag{5}$$

$$\mathbf{u} = \sum_k f_k \mathbf{c}_k / \sum_k f_k, \tag{6}$$

$$T = \sum_k g_k \tag{7}$$

The local equilibrium distribution functions for fluid flow and heat transfer are given by

$$f_k^{eq} = w_k \zeta(\mathbf{c}_k, \mathbf{u})\rho \tag{8}$$

and

$$g_k^{eq} = w_k \zeta(\mathbf{c}_k, \mathbf{u})T, \tag{9}$$

respectively, where $\zeta(\mathbf{c}_k, \mathbf{u})$ can be obtained based on the Bhatnagar-Gross-Krook (BGK) model [8] as

$$\zeta(\mathbf{c}_k, \mathbf{u}) = \left[1 + \left(\frac{\mathbf{c}_k \cdot \mathbf{u}}{3}\right) + \frac{1}{2}\left(\frac{\mathbf{c}_k \cdot \mathbf{u}}{3}\right)^2 - \frac{1}{2}\left(\frac{\mathbf{u} \cdot \mathbf{u}}{3}\right)\right]. \tag{10}$$

The corresponding dimensionless discrete velocities are

$$\mathbf{c}_k = \begin{cases} (0,0)c, & k = 0 \\ (\pm 1,0)c, & k = 1,2,3,4, \\ (\pm 1,\pm 1)c, & k = 5,6,7,8. \end{cases} \quad (11)$$

and the weighting factors are

$$w_k = \begin{cases} 4/9, & k = 0 \\ 1/9, & k = 1,2,3,4, \\ 1/36, & k = 5,6,7,8. \end{cases} \quad (12)$$

Based on the ChapmanEnskog Expansion on the dimensionless Navier-Stokes and energy equations, similar to the analysis with units [8], the relaxation times for the flow and heat transfer, and , are defined as,

Based on the ChapmanEnskog Expansion on the dimensionless Navier-Stokes and energy equations, similar to the analysis with units [8], the relaxation times for the flow and heat transfer, τ_f and τ_g, are defined as,

$$\tau_f = 3\nu_s + \frac{\Delta t}{2}, \quad (13)$$

and

$$\tau_g = 3\alpha_s + \frac{\Delta t}{2}, \quad (14)$$

The relaxation times for flow and heat transfer equations are expressed in the form of the lattice viscosity and thermal dispersivity.

The dimensionless force term due to the buoyancy force is expressed as,

$$F_k = 3w_k \mathbf{c}_k \cdot \mathbf{g}\beta\rho_f (T - T_{ref}) \quad (15)$$

where $\mathbf{g}$ is the gravity acceleration.

The dimensionless heat source term is defined as,

$$Q_k = -w_k \exp\left[\frac{-C\eta(1-\phi)(\frac{V_{porous}}{V_{tank}})t}{\left(\frac{dL^3}{\ell^2} Pr_f Ra_d\right)^{1/2}} \right] \rho c_p \Delta T \quad (16)$$

where, $\eta = \frac{A_{fs} d}{V_s}$ is a dimensionless geometry factor, defined as the ratio of the product of the microscopic length scale and the solid fluid interface area to the solid volume in are presentative elementary volume (REV),connects the macroscopic and microscopic drag and heat flux between the solid and fluid phases in a porous medium [3]. And in the present study, the shape of the heat exchangers is cylinder, thus $\eta = 4$ [3]. Based on a curve fit of prior measurements of overall heat transfer during discharge, $C = 0.26 \pm 0.01$, $\Delta T = \left(\frac{q_0}{(\rho c_p)_f} \sqrt{\frac{L}{g\beta}} \right)^{2/3}$, and $U = \sqrt{g\beta L \Delta T}$ [9, 1].

Bounce back boundary conditions are applied on the storage walls as no slip zero velocity conditions,

$$f_k = f_{k_{od}}, \quad k = 0:8 \quad (17)$$

where k_{od} is the opposite direction of k.

The temperature boundary condition for the storage tank walls are,

$$g_{k,n} = g_{k,n-1}, \quad k = 3,6,7 \quad (18)$$

The present problem is a transient problem, zero initial velocity and uniform environment temperature are selected as the initial conditions for flow and heat transfer fields. The corresponding equilibrium distribution functions are selected for the LBM scheme as,

$$f_k = w_k \rho_0, \text{ at } t = 0; \quad (19)$$

and

$$g_k = w_k T_0, \text{ at } t = 0. \quad (20)$$

Refer to the scale analysis of [1], the averaged Nusselt number for the heat transfer from the tubes to the storage tank fluid in the present study can be estimated by,

$$\overline{Nu_d} = \frac{\eta(1-\phi)(\frac{V_{porous}}{V_{tank}})\left(\frac{dL^3}{\ell^2} Pr_f Ra_d\right)^{1/2}}{(T_{porous} - T_{tank})U} \frac{\partial T_{tank}}{\partial t}. \quad (21)$$

NUMERICAL RESULTS

A computational code for the present LBM is developed in Fortran 90, which is compiled and run on the high performance computing cluster with GNU/Linux operating system (CentOS 5.5 64-bit). To maintain high accuracy, the mesh size $n \times m$ is set to be 200×1800, and the lattice size Δx is smaller than the required size for the finite difference based projection method study on the corresponding computational velocity scale [3]. Two cases shown in Fig. 1 (a) and (b) are computed to a real time length of about 1300s, which is corresponding to a discharge of 40% of total storage thermal energy.

Firstly, we would like to check the tank averaged temperature to validate the energy conservation of the LBM code. The tank averaged dimensionless temperature obtained by the present LBM simulation for geometry of the Fig. 1(a) is compared with the previous experimental study of Liu et al. (2005) and the porous medium model simulation based on finite difference based projection method of Su et al. (2007) in Fig. 2. From Fig. 2, we can see that the transient tank averaged temperature of the LBM simulation agrees very well with previous studies on for the whole discharge procedure from all of the procedure from conduction to convection. And the transient tank averaged temperature of the present LBM result and the measured results of Liu et al. (2005) are slightly higher than the porous medium model results near the turning period at time about 200s. Around this time, conduction effects decrease and convection effects begin to dominate the heat transfer.

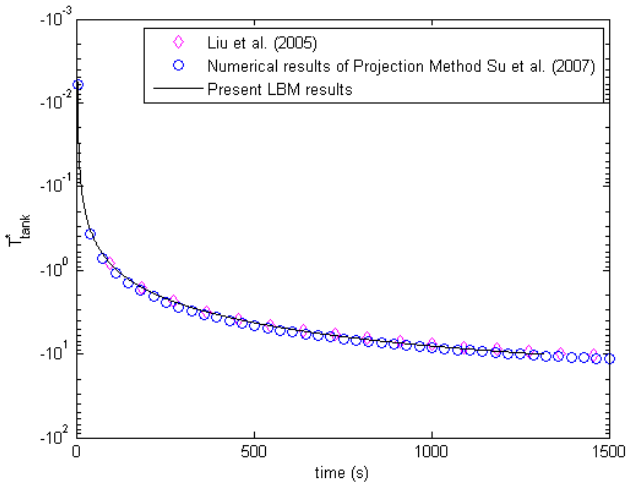

Figure 2 Transient averaged dimensionless temperature in the whole storage tank

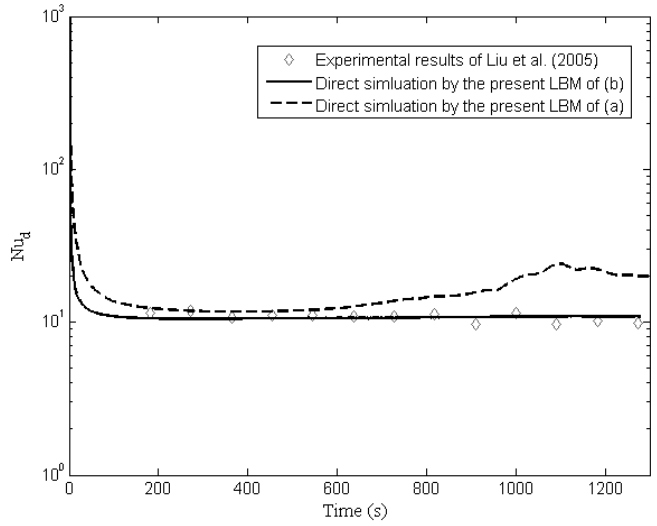

Figure 3 Transient average Nusselt numbers for the tubes

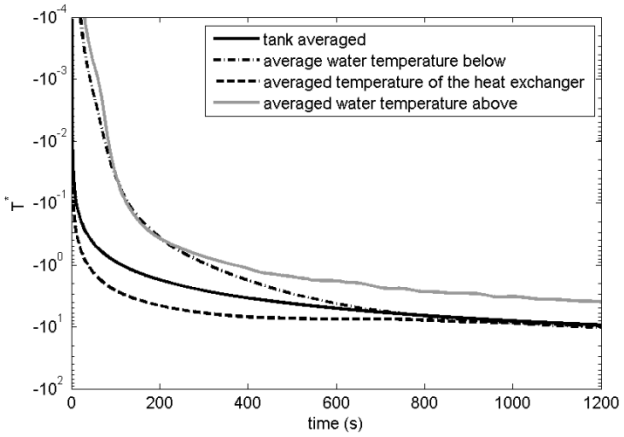

Figure 4 Transient averaged dimensionless temperature for water in, above and below the loosely distributed tube bundle

Figure 3, shows the transient averaged Nusselt number $\overline{Nu_d}$ from the present LBM results of the transient tank averaged temperature and the average temperature in the tube bundle zone based on Eq. (21). As shown in Fig. 3, the transient averaged Nusselt numbers $\overline{Nu_d}$ decay with time. They approach to a stable value near 10 for the convection dominated period, which is consistent with the porous medium study of [1] and the experimental measurement of [9]. The present direct simulation results by LBM show that the decay of the Nusselt number is quicker than the results obtained by the porous medium model, and the present predicted Nusselt numbers are more stable than those obtained by porous medium simulation. More detailed experimental studies on the initial transient heat transfer need to be done to validate the Nusselt numbers during the initial few seconds. Also the loosely packed tubes (Fig. 1(a)) has higher value of $\overline{Nu_d}$ than the compacted tubes (Fig. 1(b)) because the averaged drag is less of loosely distributed tubes, and the hot flow is more easier to enter the heat exchanger zone than the compacted case.

The average dimensionless temperature in the heat exchanger zone ($5H/9 < y < 8H/9$), below the heat exchanger zone ($0 < y < 5H/9$), and above the heat exchanger zone ($8H/9 < y < H$) are compared with the tank averaged dimensionless temperature in Fig.4. All of the four averaged temperatures drop quickly in the initial 600s, and the change of the temperature is slow down with time, which is due to the drop of the temperature difference between the tubes and the tank fluid. From Fig. 4, we can also see that the tank averaged temperature is between the average temperature of the water below the heat exchange and the average temperature in the heat exchanger zone. While the water temperature above the heat exchanger is always higher than the rest two zones, because the small stagnation zone above the heat exchange has lower velocity flow due to the buoyancy force will drive the cold plumes down along the back of the tank wall.

The transient dimensionless streamlines and isotherms at t = 700 s are plotted in Fig. 5 and 6 respectively. The bottom parts of the pictures present the contour plot in full tank and the top parts of the pictures present for zoom pictures in the zone filled tubes. Figure 5 shows that both the large scale flows and the detailed flow around the tubes can be shown in the present LBM method results. The velocity in the pure fluid zone is higher than the velocity in the tube bundle zone due to the drag of the tube bundle heat exchanger. Figure 6 shows that the temperature distributions in both large scale inside the tank and the detailed distributions near each tube are clearly shown either.

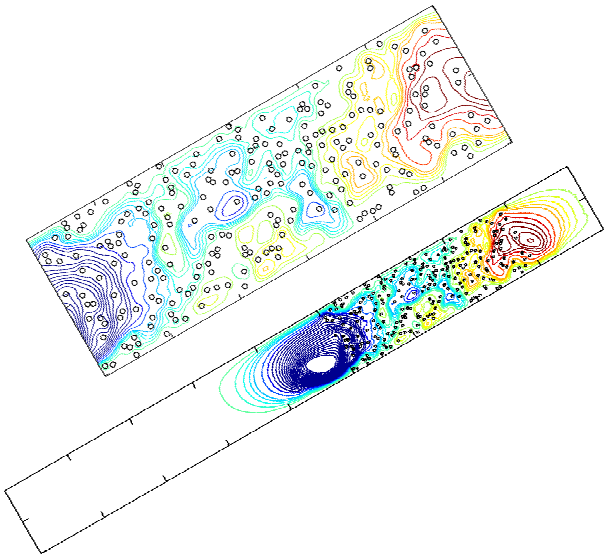

Figure 3 Contour plot of streamlines at 12s: bottom picture for full tank and top picture for zoom in the loosely packed tubes

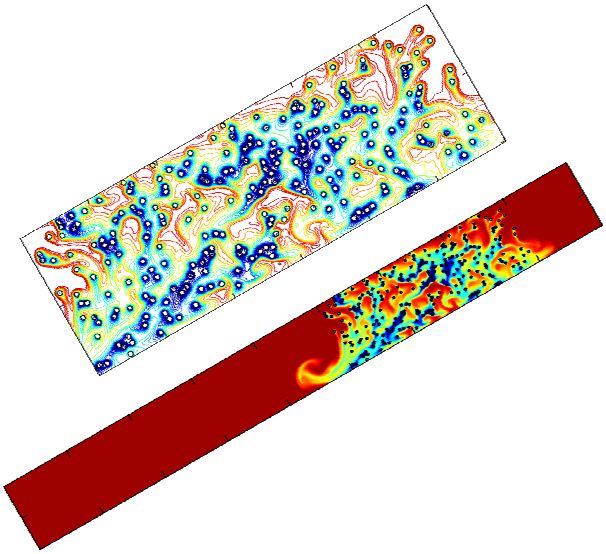

Figure 4 Contour plot of isotherms at 12s: bottom picture for full tank and top picture for zoom in the loosely packed tubes

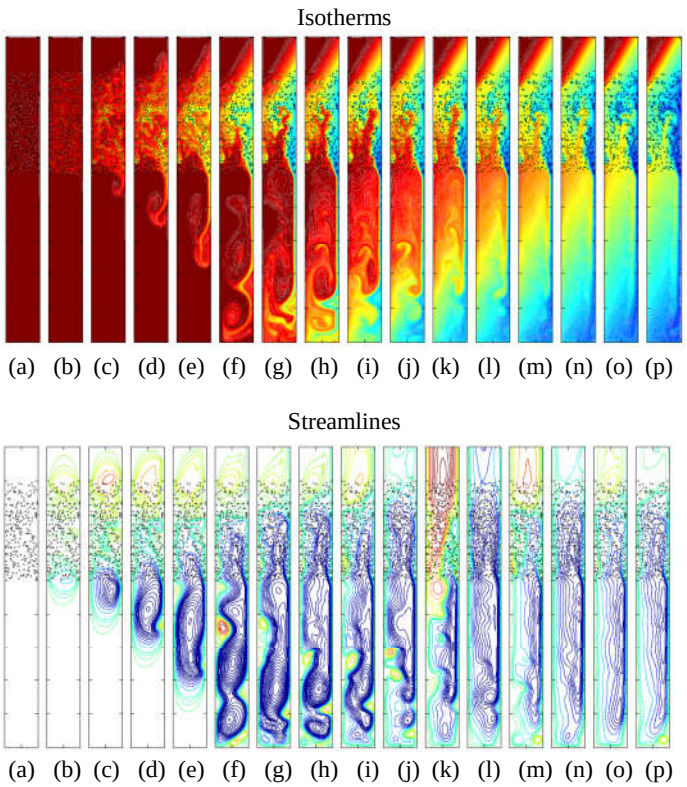

Figure 7 Transient isotherms and streamlines of loosely distributed tubes for the initial 1300s

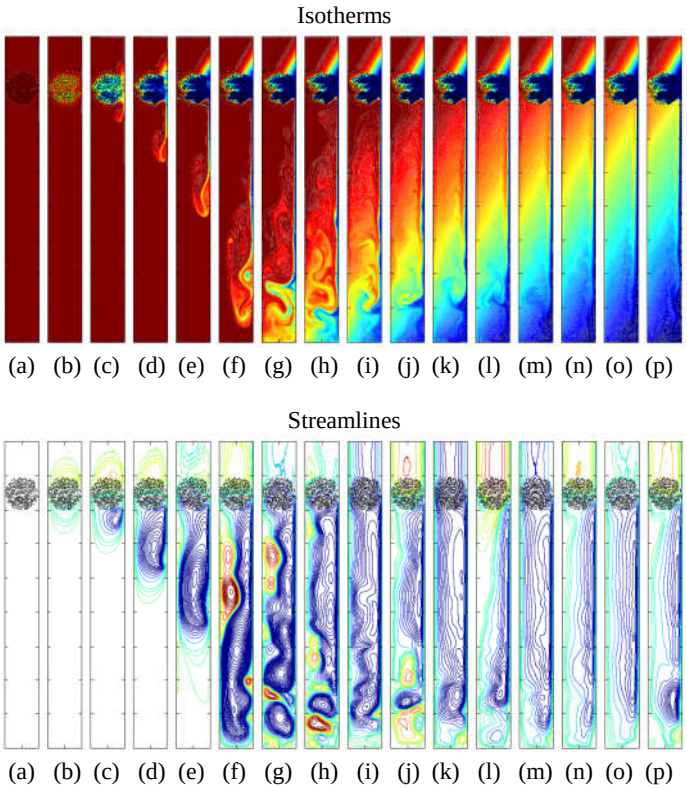

Figure 8 Transient isotherms and streamlines of compacted tubes for the initial 1300s

Figure 7 and 8 present the transient isotherms and streamlines of the initial 1300s for the loosely distributed tubes and the compacted tubes, respectively. From Fig. 7, we can see that the tank temperature decay with time and there are stratifications of thermal fluid along the gravity direction, which was not observed so clearly in the porous medium model simulations of Su et al. (2007). Figure 7 (a) and (b) show that the heat transfer is initially dominated by conduction when time is small. Figure 7(c) show that the cold thermal plume initially generated along the tube walls and the main cold plume drops down along the back wall, which is consistent with the porous medium simulation of Su et al. (2007). Then mushroom structure cold plumes generated as shown in Fig. 7 (c) and (d). And the mushroom structure will be destroyed based on the thermal dispersion inside water under the heat exchangers. When reach the bottom of the tank, the cold plume will bump back from the bottom wall as shown in Fig. 7(e). Shown in Fig. 7(f) and (g), although the cold plume drops down from the back wall, the hot water will be pushed back into the heat exchanger zone from middle part of the heat exchangers. This phenomenon was not observed by the previous porous medium model study. Blue colored cold plume begin to reach the bottom of the tank and stay there due to buoyancy force as shown in Fig. 7 (h) and (i). Then the cold plumes bump back before they reach the bottom of the tank because high density cold water will be staged at right bottom corner. After that the tank is more stratified and the velocities of fluid in the tank decay with time, as shown in Fig. 7 (m) to (p). This is also due to the temperature difference between the solid wall and the tank water decrease with time. There is large scale fluid motion under the heat exchanger tubes while the fluid is almost staged above the heat exchanger tubes. And inside the heat exchanger, the fluid flow directions highly depend on the distribution of the tubes. Figure 8 shows the similar heat transfer procedure as those in Fig.7, excepting that the time is delayed in the conduction period. And the stratification of the storage is more obvious.

CONCLUSION

LBM simulations for discharge procedure of a randomly distributed 240 tube bundle heat exchange immersed near the top of a solar storage tank have been done. The transient tank averaged temperature and the averaged Nussult numbers decay with time and agree with previous experimental and numerical study in finite difference based projection method. The macroscopic, microscopic, and mesocopic length scales are defined from length scales of the storage tank, the small tube diameter, and the mesh size respectively. The present LBM results clearly show both macroscopic and microscopic transient flow and temperature distributions.

ACKNOWLEDGEMENT

The present study was supported by FDCT/115/2012/A, MYRG151(Y1-L2)-FST11-SY, and MYRG080(Y1-L2)-FST13-SY.

REFERENCES

[1] Su Y. and Davidson, J.H., Multi-zone Porous Enclosure Model of Thermal/Fluid Processes during Discharge of an Inclined Rectangular Storage Vessel via an Immersed Heat Exchanger, ASME J. of Solar Energy Engineering, 129, 449-457, 2007.

[2] Luan H.B., Xu H., Chen L., Sun D.L., He Y.L., Tao W.Q. (2011) Evaluation of the coupling scheme of FVM and LBM for fluid flows around complex geometries. International journal of heat and mass transfer, 54: 1975-1985.

[3] Su Y., Davidson, J.H., Kulacki, F.A., A Geometry Factor for Natural Convection in Open Cell Metal Foam, International Journal of Heat and Mass Transfer, 2013; 62(1):697-710

[4] Guo Y., Bennacer R., Shen S., Ameziani D.E., Bouzidi M. (2010) Simulation of mixed convection in slender rectangular cavity with lattice boltzmann method. International journal of Numerical methods for Heat & fluid flow, 20 (1), pp 130-148.

[5] Mondal B., Mishra S.C. (2009) Simulation of natural convection in the presence of volumetric radiation using the Lattice Boltzmann Method. Numerical Heat Transfer, Part A, 55, 18-41.

[6] Lai F.H., Yang Y.T. Lattice Boltzmann simulation of natural convection heat transfer of Al O /water nanofluids in a square enclosure. International journal of thermal sciences. 50: 1930-1941.

[7] Mehrizi A.A., Farhadi, M., Afroozi, H.H., Sedighi K., Darz A.A.R. (2012) Mixed convection heat tranfer in a ventilated cavity with hot obstacle: effect of nanofluid and outlet port location. 39: 1000-1008.

[8] Tarokh A., Mohamad A.A., Jiang L. (2013) Simulation of conjugate heat transfer using the lattice boltzmann method. Numerical Heat Transfer, part A, 63:159-178.

[9] Liu, W. Davidson, J.H., Kulacki, F.A., and Mantell, S. C., 2003. Natural Convection from a horizontal tube heat exchanger immersed in a tilted enclosure, Journal of Solar Energy Engineering, 124,1, 67-75.